Water Research 257 (2024) 121677

Contents lists available at ScienceDirect

Water Research

journal homepage: www.elsevier.com/locate/watres

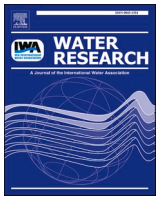

Direct and indirect photodegradation in aquatic systems mitigates photosensitized toxicity in screening-level substance risk assessments of selected petrochemical structures

Davide Vione [a,**], J. Samuel Arey [b], Thomas F. Parkerton [c], Aaron D. Redman [d,*]

[a] Department of Chemistry, University of Torino, Via Pietro Giuria 5, 10125 Torino, Italy
[b] Oleolytics LLC, State College, PA, USA 16801
[c] EnviSci Consulting LLC, Austin, TX, USA 78731
[d] ExxonMobil Biomedical Sciences, Inc Annandale, NJ USA 08801

ARTICLE INFO

Keywords:
Photodegradation
Phototoxicity
Photosensitization
Aquatic Risk Assessment
Petrochemicals

ABSTRACT

Photochemical processes are typically not incorporated in screening-level substance risk assessments due to the complexity of modeling sunlight co-exposures and resulting interactions on environmental fate and effects. However, for many substances, sunlight exerts a profound influence on environmental degradation rates and ecotoxicities. Recent modeling advances provide an improved technical basis for estimating the effect of sunlight in modulating both substance exposure and toxicity in the aquatic environment. Screening model simulations were performed for 25 petrochemical structures with varied uses and environmental fate properties. Model predictions were evaluated by comparing the ratios of predicted exposure concentrations with and without light to the corresponding ratios of toxicity thresholds under the same conditions. The relative ratios of exposure and hazard in light vs. dark were then used to evaluate how inclusion of light modulates substance risk analysis. Results indicated that inclusion of light reduced PECs by factors ranging from 1.1- to 63-fold as a result of photodegradation, while reducing PNECs by factors ranging from 1- to 49-fold due to photoenhanced toxicity caused by photosensitization. Consequently, the presence of light altered risk quotients by factors that ranged from 0.1- to 17-fold, since the predicted increase in substance hazard was mitigated by the reduction in exposure. For many structures, indirect photodegradation decreases environmental exposures independently of the direct photolysis pathway which is associated with enhanced phototoxicity. For most of the scenarios and chemicals in the present work, photosensitization appears to be mitigated by direct and indirect degradation from sunlight exposure.

1. Introduction

Screening-level risk assessments are used as an assessment tool in chemicals management to integrate the combined effect of environment processes with the physicochemical properties of a substance (Mackay, 2001). Historically, the role of light has not been widely considered in multimedia models used for risk assessments, due to the complexity and site-specific nature of modeling light co-exposures and the influence such light interactions pose on degradation and toxicity of a substance (CONCAWE, 2013, 2020). However, it is known that light has a profound impact on the fates (Boreen et al., 2003; Fasnacht and Blough, 2003) and toxicities (Alloy et al., 2023; Björn and Huovinen, 2015) of some organic chemicals. For certain chemicals that do not biodegrade rapidly, direct and indirect photodegradation can represent the predominant transformation process in shallow water bodies such as ponds, rivers, embayments, or wetlands (Bonvin et al., 2013; Guerard et al., 2009; Jasper and Sedlak, 2013; Werner et al., 2005). Direct and indirect photodegradation of some commercial chemicals can also produce transformation products that are more ecotoxic than the parent (Albanese et al., 2017; Latch et al., 2005; Zhao et al., 2023), which further illustrates the importance of characterizing the susceptibility of chemicals to photochemistry. Recent advances in modeling phototoxicity (Marzooghi and Di Toro, 2017; Marzooghi et al., 2017) and photodegradation (Bodrato and Vione, 2014) provide a technical basis for

* Corresponding author.
** Corresponding author.
E-mail addresses: davide.vione@unito.it (D. Vione), aaron.d.redman@exxonmobil.com (A.D. Redman).

https://doi.org/10.1016/j.watres.2024.121677
Received 15 February 2024; Received in revised form 22 April 2024; Accepted 23 April 2024
Available online 24 April 2024

evaluating the combined effect of light in modulating both substance exposure and hazard, and the resulting risk of chemicals in the aquatic environment.

The objective of this work is to apply screening models to characterize the role that light serves in modulating the aquatic risks of selected chemicals in a representative environmental scenario, given the recognized importance of light as key modifying environmental variable (Loiselle et al., 2012; Remucal, 2014; Rosario-Ortiz and Canonica, 2016; Yan and Song, 2014). The present study used a combination of mechanistic photodegradation and phototoxicity models to quantify the magnitude that light co-exposures alter screening-level environmental risk evaluations when compared to assessments that ignore substance-light interactions. These processes are depicted in Fig. 1 and described in more detail in the following paragraphs.

Photodegradation can be represented as the combined effects of direct photolysis, in which the parent substance transforms due to absorption of light, and indirect photodegradation, which is mediated by reaction with radicals and other transients formed from the interaction of UV light with aquatic constituents including dissolved organic carbon, or major ion species (Schwarzenbach et al., 2016). In some cases indirect photodegradation can represent the dominant fate pathway for certain pollutants, depending on the environmental conditions (Jasper and Sedlak, 2013; Remucal, 2014; Zeng and Arnold, 2013) and is characterized by reactions with photochemically-produced reactive intermediates (PPRIs), such as the hydroxyl ($^{\bullet}OH$) and carbonate ($CO_3^{\bullet-}$) radicals, the excited triplet states of chromophoric dissolved organic matter ($^3CDOM^*$), and singlet oxygen ($^1O_2$) (Brezonik and Fulkerson-Brekken, 1998; Vione and Scozzaro, 2019). The steady-state concentrations of PPRIs are closely related to sunlight irradiance, water depth, and water quality conditions. Typically, $^{\bullet}OH$ is photochemically generated in sunlit freshwaters by irradiation of nitrate, nitrite, and chromophoric dissolved organic matter (CDOM), and it is mainly scavenged by dissolved organic matter (DOM, not necessarily chromophoric), bicarbonate, and carbonate. The triplet states $^3CDOM^*$ are produced by irradiated CDOM and mostly quenched by dissolved O_2, partially to produce $^1O_2$ with ~50 % yield (Janssen et al., 2014; McNeill and Canonica, 2016). The main quenching pathway of $^1O_2$ is collision with the water solvent. Finally, $CO_3^{\bullet-}$ is generated upon HCO_3^-/CO_3^{2-} oxidation by $^{\bullet}OH$ and CO_3^{2-} oxidation by $^3CDOM^*$, and it is mostly scavenged by DOM (Yan et al., 2019). Moreover, considering that CDOM is a key sunlight absorber and competes with substances evaluated in risk assessments for sunlight irradiance and, therefore, for the direct photolysis (Bianco et al., 2015), there is a clear link between water quality conditions and photodegradation kinetics.

The present study focused on the role of the parent molecules. For example, overall toxicity of irradiated PAH in aqueous solution is observed to decrease following irradiation since the phototransformation products are less toxic than the parent molecules (Kang et al., 2019; Nordborg et al., 2023). However, for certain molecules like phenolic anti-oxidants the phototransformation products could include reactive molecules like quinones (Vione et al., 2007), which could be more toxic than the parent molecules, which was out of scope for the present modeling study.

A mechanistic effect model was used to simulate the enhanced toxicity through the absorption of light by the biologically absorbed chemicals (i.e., photosensitization). This model translates the total amount of photons absorbed by the bioaccumulated test substance to toxicity using empirically derived parameters that account for generation of reactive products in organism tissues to predict excess toxicity relative to dark conditions (Finch et al., 2017; Marzooghi et al., 2018). In the present study, photosensitization refers to toxicity that occurs when molecules absorb light while occurring in biological tissues. This appears to be the principal mechanism of toxicity responsible for observed photoenhanced toxicity of aromatic hydrocarbons and petroleum products (Alloy et al., 2023; Ankley et al., 1997; Sellin Jeffries et al., 2013). The mechanism of photosensitization is likely due to the photoexcitation of a molecule that is bioaccumulated, and this excitation would lead to the formation of reactive intermediates in the organism that are responsible for the enhancement of toxicity (Alloy et al., 2023; Marzooghi et al., 2018).

A one-box exposure model was used to illustrate the relative impact of light using a hydraulic retention time typical of large European rivers

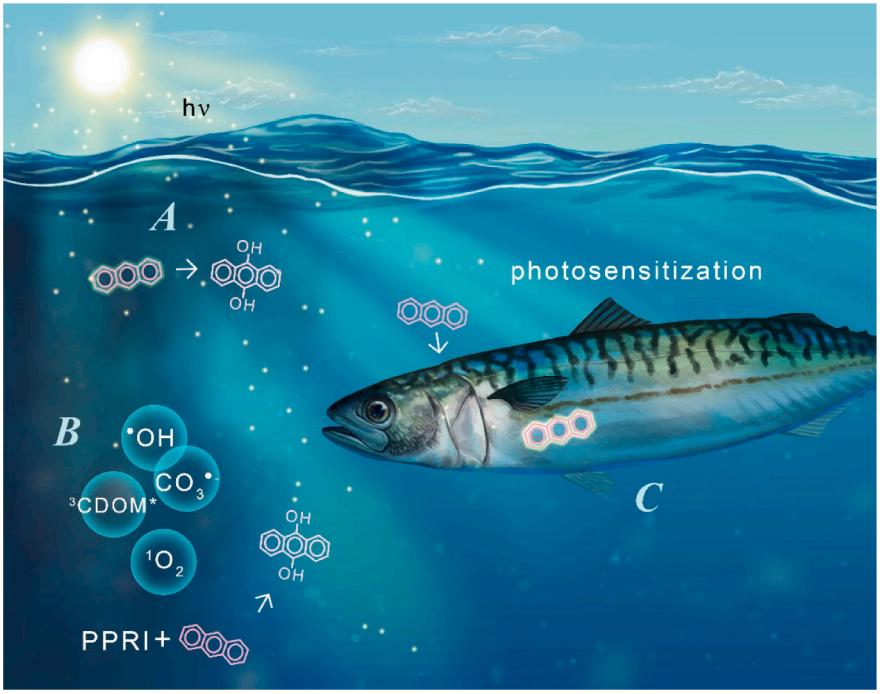

Fig. 1. Conceptual model of the major processes being evaluated in the present study: **A)** direct photolysis where an aromatic molecule absorbs light that induces a chemical reaction, **B)** Indirect photolysis through reaction of organic chemicals with photochemically-produced reactive intermediates (PPRIs), and **C)** photosensitization where a molecule that was absorbed by an organism absorbs photons that induces a chemical reaction that causes excess toxicity in aquatic organisms.

(Van de Meent et al., 2000). Simulations were performed by comparing the ratios of predicted exposure concentrations (PECs) in light and dark exposures to the corresponding ratios for predicted toxicity thresholds (predicted no-effect concentrations, PNECs) under analogous light and dark conditions. The relative ratios of exposure and toxicity with and without light then provided the basis for evaluating the relative impact of light on the estimated risk ratios (e.g.,. ratios of PEC and PNEC).

2. Methods

2.1. Chemical domain

The 25 test substances included aliphatic and aromatic hydrocarbons that are representative constituents in petroleum products, intermediates used in chemicals manufacture as well as additives in finished products (i.e. antioxidants, plasticizers). The selected structures span a range of physicochemical properties, including toxicity and degradability, and photoreactivity. Some are naturally occurring, and some are additives to improve performance of commercial products. These substances span a wide range in partitioning properties (e.g. log K_{ow} from 2.5 to 13.1), estimated biodegradation half-lives (e.g. 4 to 246 days) and susceptibilities to photoreactivity in aquatic systems. The chemical names, CAS numbers, SMILES strings, chemical structures, log octanol water and log octanol air partition coefficients, estimated aerobic biodegradation half-lives in water, and typical commercial uses are provided in **Table S1**. Substances with aromatic functional groups absorb light and are susceptible to both direct photolysis and photosensitization in water. By contrast, all test substances are potentially susceptible to indirect photodegradation, which includes reactions with both selective ($CO_3^{\bullet -}$, ^{3}CDOM*, and $^1O_2$) and non-selective oxidants ($^\bullet$OH).

2.2. Sunlight

Sunlight exposures used in this work (Vione and Carena, 2022) are representative of typical mid-latitude weather conditions in Europe, are similar to those experienced in Torino, NW Italy (45°N), and were expressed as spectral photon flux density $p^\circ(\lambda)$ in units of Einstein cm^{-2} s^{-1} nm^{-1} (Einstein=mol photons). Data are based on spectroradiometer measurements, with spectral resolution ranging from 2.5 nm in the UVB region to 10–25 nm in the visible. To evaluate temporal changes in sunlight exposures, irradiance was compiled on the 15th day of each month. The annual average $p^\circ(\lambda)$ over 280 to 700 nm at the water surface was 64.8 Einstein m^{-2} d^{-1}. Light exposures varied seasonally from 18.8 in December to 102.2 Einstein m^{-2} d^{-1} in August. The average $p^\circ(\lambda)$ in the UVB, UVA and visible range was 0.13, 4.5, and 60.9 Einstein m^{-2} d^{-1}, respectively. For comparison, the light exposures assumed in this work are approximately 1.5X higher than reported for the Gulf of Mexico which averaged approximately 40 with a seasonal range of 10 to 60 Einstein m^{-2} d^{-1} (Ward et al., 2018). The values of $p^\circ(\lambda)$ decrease exponentially with depth, mostly due to radiation absorption by CDOM within the water column. See Appendix A1 for calculation method (Supplementary Material).

2.3. Photolysis in aquatic systems

Photodegradation kinetics of the test compounds were assessed by considering both direct photolysis (when applicable) and indirect photochemistry. Water quality characteristics were assumed that are representative of mid-latitude water bodies, which include DOC (dissolved organic carbon) = 3 mg_C L^{-1}, $[NO_3^-] = 10^{-4}$ M, $[NO_2^-] = 10^{-6}$ M, $[HCO_3^-] = 10^{-3}$ M, and $[CO_3^{2-}] = 10^{-5}$ M (Minero et al., 2007; Reinart et al., 2004; Vione et al., 2010). Note that, in these conditions, $[CO_3^{2-}]/[HCO_3^-] = 10^{-2}$ result in pH ~ 8. The concentration of bromide was here considered negligible; in a majority of surface waters $[Br^-] < 10^{-6}$ M (Magazinovic et al., 2004; Soltermann et al., 2016), which in our case means that Br^- could scavenge <10 % $^\bullet$OH. In addition, a 3 m water depth was used to reflect the default value assumed in the EUSES multimedia model used for regional substance risk assessments (Den Hollander et al., 2004). These data were input to the APEX (Aqueous Photochemistry of Environmentally-occurring Xenobiotics) software tool. In addition to water quality data and depth, APEX requires substance-specific photoreactivity parameters to assess photodegradation kinetics. These parameters include absorption spectra, direct photolysis quantum yields, and second-order reaction rate constants with PPRIs.

2.3.1. Direct photolysis in aquatic systems

Pseudo-first order rate constants for the direct photolysis ($k_{d.p.}$, day^{-1} units) were computed for each light absorbing test substance using the following equation:

$$k_{d.p.} = 1000\ \Phi \int_{\lambda_1}^{\lambda_2} \left[p^{\circ -3}(\lambda)\, \varepsilon(\lambda)\, \tau\right] d\lambda = \Phi\, P_{abs} \quad (1)$$

where $p^{\circ -3}(\lambda)$ [Einstein cm^{-2} s^{-1} nm^{-1}] is the spectral photon flux density of sunlight integrated over a 3 m depth calculated using Eq. A1, Φ [mol chem transformed $Einstein^{-1}$] is the direct photolysis quantum yield of the chosen compound, $\varepsilon(\lambda)$ [L mol $chem^{-1}$ cm^{-1}] it's the wavelength-dependent molar absorption coefficient and τ = 43,200 s day^{-1} which accounts for the 12-h averaging period of sunlight exposures consistent with the annual average daylight duration at mid latitude.

Annual average estimates of $p^{\circ -3}(\lambda)$ at 1 nm intervals are provided in Table S2 and were used to calculate direct photolysis rates on a yearly basis. Monthly $p^{\circ -3}(\lambda)$ estimates are also reported to allow seasonal variation in light exposures on direct photolysis to be examined. For each test substance with an expected chromophoric group, $\varepsilon(\lambda)$ was determined whenever possible by direct absorption measurements of standard solutions, from literature values or experimentally determined as part of this study (see Section A2). Similarly, $\Phi_{d.p.}$ were taken from the literature when available, or assumed to be reasonably approximated by literature values for related compounds. The quantum yields and absorption spectra used for calculations are reported in Table S3 and Table S4, respectively. Since none of the test substances appreciably absorb visible light, Eq. (1) was applied over only UV wavelengths, i.e. λ_1=280 and λ_2=400 nm. An example illustration is given in Fig. A1.

2.3.2. Indirect photodegradation in aquatic systems

APEX computes radiation absorption by photosensitizers (CDOM, nitrate, nitrite) by means of Eq. (2) having the following form (S = sensitizer molecule with concentration [S]; $A(\lambda)$ = absorbance of water per unit path length [cm] and unit DOC [mg_C L^{-1}]); in the case of CDOM that absorbs nearly all radiation between 280 and 500 nm, it was assumed $\frac{\varepsilon(\lambda)\,[S]}{A(\lambda)\,DOC} \sim 1$:

$$P_{abs,S} = \frac{10}{d} \int_{\lambda_1}^{\lambda_2} \left[p^\circ(\lambda)\, \frac{\varepsilon(\lambda)\,[S]}{A(\lambda)\,DOC} \left(1 - 10^{-100\, A(\lambda) y\, DOC\, d}\right)\right] d\lambda \quad (2)$$

Radiation absorption by photosensitizers allows for calculating PPRIs formation rates from known quantum yield values; then, steady-state concentrations of PPRIs are determined by dividing formation rates by the scavenging rate constants (Vione, 2020).

The second-order reaction rate constants of the test substances with PPRIs (Table A3 in Appendix) were assessed as follows. To estimate the second-order rate constants of test substances with the hydroxyl radical ($^\bullet$OH), known correlations were applied between gas-phase and water-phase reaction kinetics (Gligorovski et al., 2015) (Appendix A3). The gas-phase reaction kinetics with $^\bullet$OH were estimated with the AOPWIN application of EPIWEB (EPI Suite v4.10). To estimate the second-order rate constants of the test chemicals with $CO_3^{\bullet -}$, ^{3}CDOM*, and $^1O_2$, we developed new correlations between previously measured rate constant

values and the quantum-chemical computed one-electron oxidation potentials, E_{ox}, for an independent training set of 21 chemicals (Table A1, Appendix A3), analogous to the approach used by Arnold and coworkers for phenols (Arnold et al., 2017).

The individual and overall indirect rates are listed in Table S6. Considering the uncertainties associated with the assessment of reaction rate constants and quantum yields, as well as those connected with photochemical modeling with APEX, the first-order photodegradation rate constants thus obtained should be regarded as order-of-magnitude estimates.

2.4. Aquatic phototoxicity

Phototoxicity was modeled using the photo Target Lipid Model (pTLM), which is a QSAR that predicts the photo-enhanced toxicity due to photosensitization (Marzooghi and Di Toro, 2017; Marzooghi et al., 2017). The reader is referred to those papers for the full derivation. Since our study focused on the relative impact of light on toxicity, we relied on an adaptation of Eqn 25 from Marzooghi et al. (2017):

$$\frac{\mathrm{PLC50}}{\mathrm{NLC50}} = \frac{1}{1+\frac{(P_{abs})^{\alpha}}{R^{'*}}} \tag{3}$$

where the ratio of photo-enhanced toxicity (PLC50) to the toxicity in dark (NLC50) is related to the absorbed photons, P_{abs}, divided by $R^{'*}$, an empirical relative toxicity scaling parameter. In this context "dark" refers to a typical toxicity exposure where exposure to UV light is minimized to avoid photosentitization. The absorbed photons, P_{abs} in units of mols photons absorbed/mol chemical absorbed over a daily exposure period, are calculated by summing the product of the wavelength-dependent and depth-integrated light exposure, the molar absorption of the test substance over the UV as described previously in Eq. A1. The relative toxicity scaling parameter, $R^{'*}$, and exponent on the photon absorption term, α, were derived by fitting this model framework to empirical toxicity data for PAHs (Marzooghi et al., 2017). It is assumed that this framework is generally applicable to other aromatic organic molecules. In the present study P_{abs} was calculated with the light intensity (Table S2) and the absorption spectra for the test substances (Table S4) between wavelengths of 280 nm to 400 nm consistent with the procedure used for estimating direct photolysis.

2.5. Comparison of acute and chronic thresholds without light

Phototoxicity is generally considered a short term, acute toxicity issue. Acute toxicity testing is often performed at relatively high concentrations, and high light intensities over short durations (<2d). Chronic testing is performed at lower concentrations, typically by factors of 5–20, see McGrath et al., (2018) for description of acute and chronic toxicity data for hydrocarbons. At lower exposures the ability of organisms to undergo repair of the photo-induced damage is an important factor (Williamson et al., 2011; Williamson et al., 2001) that has not been broadly considered. Therefore, a second evaluation criterion is presented to compare the relative change in risk due to light exposure to the ratio of acute to chronic PNECs in the dark, since the chronic dark threshold is commonly used in general purpose risk assessment. See example given in Parkerton et al., (2023), where photoenhanced toxicity in mixture exposures is demonstrated to be less than or equal to the standard chronic toxicity thresholds, which are not based on phototoxicity. The average ratio of acute to chronic thresholds for hydrocarbons is 21, which is used in the analysis below as the benchmark for classic risk evaluations (e.g., without photosensitization).

2.6. Exposure model

A one box exposure model was parameterized using typical regional parameters for Europe (Den Hollander et al., 2004). Specifically, we assume a 3 m depth for a freshwater river, a freshwater volume of 3.6×10^9 m^3, and a flow of 8.31×10^7 m^3/d, which results in an average residence time (τ) of 43.3 days.

The relative concentrations (C_{light} vs. C_{dark}) were calculated as the ratio of the steady state concentrations based on estimated biodegradation rates (k_{bio}) from HCBioSim in Davis et al., (2022) for hydrocarbons and OPERA for the remaining chemicals (Mansouri et al., 2018) with, or without the combined direct and indirect photodegradation rates (k_{photo}). The estimated biodegradation rates should be viewed as order-of-magnitude estimates, given the uncertainties of the predictive models and expected variability in environmental conditions. The relative concentrations were calculated as:

$$\frac{C_{light}}{C_{dark}} = \frac{1+\tau\, k_{bio}}{1+\tau\left(k_{bio}+k_{photo}\right)} \tag{4}$$

Where τ is the residence time of water. Derivation of this model is given in the supplementary information (Appendix A4) and is based on a 1-box model.

3. Results

3.1. Aquatic photodegradation rates

The modeling analysis in the present study considered both direct and indirect photodegradation pathways. Among the studied compounds, direct photolysis is only relevant for substances with aromatic ring structures that absorb sunlight. The magnitude of the predicted direct photolysis rates ranges from ca. 0.001 d^{-1} for substances like dibenzothiophene, to >1 d^{-1} for anthracene, benzo[a]pyrene, and phenylamine, Table S6, Table 1.

Since indirect photodegradation rates depend on reaction with PPRIs generated from light interactions with constituents in the water column, predicted rates are not correlated to photon absorption by the contaminants. The magnitude of the indirect rates ranges from around 0.003 d^{-1} to 0.2 d^{-1}, which is similar to the range of estimated biodegradation rates (Table S6). Total degradation rates (sum of biodegradation, direct and indirect photolysis rates) are illustrated in Fig. 2, showing the relative contributions of direct photolysis, indirect photodegradation, and biodegradation. The horizontal axis in the figure compares the total rates to the product of QY × Pabs, which is an estimate of the susceptibility of each compound to the direct photolysis process and has units of moles of reacted chemical within the exposure period per moles of parent substance. The alkyl trimellitate (ID 19) and the alkyl anisole (ID7) show low photoreactivity due to their very low Pabs (<0.004), despite their relatively high QY (>0.01).

Direct photolysis rates (light blue segments of symbols in Fig. 2) are typically faster than indirect photodegradation rates (purple segments) and biodegradation rates (red segments), for the petrochemicals and environmental conditions considered in the present study. The modeled direct photolysis rates are correlated with the product of the QY and Pabs, which is the mechanistic basis of the direct photolysis reaction. By contrast, neither biodegradation rates nor indirect photodegradation rates were found to correlate with direct photolysis rates, nor with each other. Interestingly, the molecular features that can produce fast biodegradation appear to be quite different from those favoring photodegradation. For instance, the considered PAHs undergo rapid photodegradation, often outcompeting biodegradation rates, as these molecules contain extended aromatic groups which are effective chromophores (direct photolysis) and also represent electron-rich sites of attack for PPRIs (indirect photodegradation). Terphenyl and the multiring structures containing a mixture of aliphatic and aromatic rings (dehydroabietine, dodecahydrochrysene and hexahydropyrene) exhibit consistent susceptibilities to indirect photodegradation, but widely varying rates of direct photolysis and biodegradation.

The electron-rich substituted phenols exhibited comparable rates of

Table 1
Summary of ID number (an index), chemical name, logKow, and estimated biodegradation and photodegradation rates (yearly averages) considered in the present study.

ID#	Substance	log Kow	Biodeg k (1/d)	Photo_indirect (1/d)	Photo_direct (1/d)	TotalPhotodeg k (1/d)
1	decalin	4.2	5.70E-02	1.08E-02	0.00E+00	1.08E-02
2	3-methylphenanthrene	4.89	7.04E-02	5.05E-02	6.82E-03	5.73E-02
3	benzofuran	2.54	8.82E-02	3.58E-02	0.00E+00	3.58E-02
4	dicyclopentadiene	3.16	5.14E-02	4.18E-02	0.00E+00	4.18E-02
5	trimethyldecanol	5.08	1.42E-01	6.90E-03	0.00E+00	6.90E-03
6	dibutyladipate	4.33	1.22E-01	5.38E-03	0.00E+00	5.38E-03
7	alkylated anisole	5.46	1.53E-01	5.75E-02	3.95E-02	9.70E-02
8	2,4,6 tri-tert-butylphenol	6.39	3.52E-02	7.50E-02	1.43E-02	8.93E-02
9	4,4′ ditertbutyldiphenylamine	7.11	3.43E-02	2.67E-01	3.38E+00	3.65E+00
10	dodecahydrochrysene	6.24	5.70E-02	4.55E-02	0.00E+00	4.55E-02
11	dehydroabietine	7.76	5.66E-03	3.57E-02	6.08E-04	3.63E-02
12	2,6 diisopropylnaphthalene	6.08	7.58E-02	5.38E-02	9.35E-03	6.32E-02
13	hexahydropyrene	6.12	1.11E-01	1.28E-01	1.90E-01	3.18E-01
14	o-terphenyl	5.52	5.70E-02	2.80E-02	9.70E-04	2.90E-02
15	dihydrodicyclopentadiene	3.38	9.04E-03	3.45E-02	0.00E+00	3.45E-02
16	bicyclo[4.1.0]heptane-7-ylidenecyclopentane	6.37	2.80E-03	6.12E-02	0.00E+00	6.12E-02
17	tris(4-isopropylphenyl)-phosphate	9.07	1.63E-01	2.43E-02	0.00E+00	2.43E-02
18	2,4-di-tert-butylphenol	5.33	6.78E-02	6.67E-02	7.39E-02	1.41E-01
19	triisononyl trimellitate	13.06	1.63E-01	1.00E-02	3.88E-01	3.98E-01
20	tetradecylnaphthalene	10.03	1.31E-01	5.98E-02	6.78E-02	1.28E-01
21	anthracene	4.35	1.11E-01	8.33E-03	9.13E-01	9.22E-01
22	fluoranthene	4.91	7.84E-02	6.67E-03	2.63E-02	3.30E-02
23	pyrene	4.93	6.27E-02	1.00E-02	4.47E-01	4.57E-01
24	benzo[a]pyrene	6.11	4.34E-02	3.17E-02	1.16E+00	1.19E+00
25	dibenzothiophene	4.17	4.57E-02	2.31E-02	6.85E-04	2.38E-02

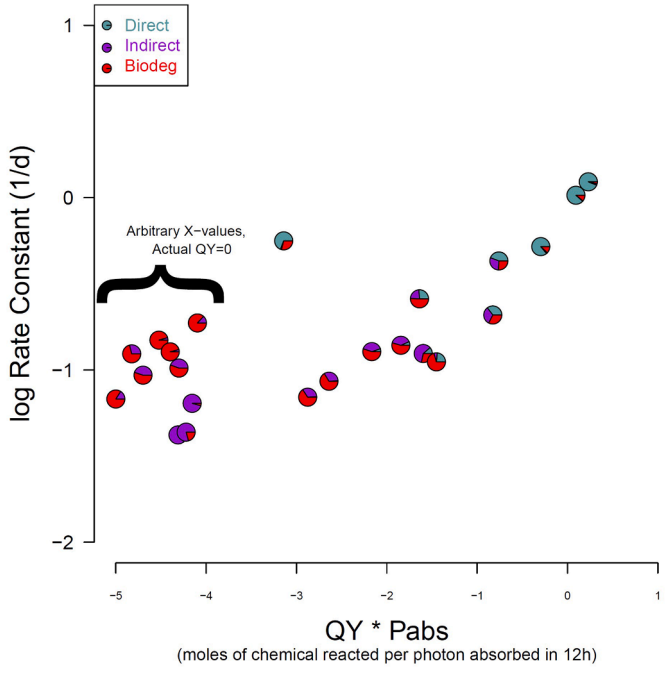

Fig. 2. The sum of all first order degradation rate constants for Direct photolysis (blue), Indirect photodegradation (purple), and Biodegradation (red) compared to the product (Log_{10} value) of the Quantum Yield (Table S1), and the Photon absorption in a 12 h period (Table S5) for typical light intensity and duration (year averages) in Torino, Italy. Substances with QY*Pabs=0 are plotted arbitrarily at a low value (<1e-4) for visual comparison.

photodegradation and biodegradation, with indirect photodegradation representing the dominant phototransformation mechanism in some cases. Among the structures containing carboxylic groups (dibutyladipate and tri-isononyl trimellitate), predicted biodegradation rates dominate over modeled photodegradation rates. The aromatic amine (4,4′ di-*tert*-butyldiphenylamine) exhibited rapid rates of both direct photolysis and indirect photodegradation, outcompeting biodegradation. The diene structures (dicyclopentadiene, dihydrodicyclopentadiene, and bicyclo[4.1.0]heptane-7-ylidenecyclopentane) exhibit roughly comparable susceptibilities to both biodegradation and to indirect photodegradation, but they do not react by direct photolysis. Finally, saturates (e.g., decalin) have generally comparable rates of biodegradation and indirect photodegradation.

3.2. *Characterization of direct and indirect photodegradation*

There are interesting differences between compounds undergoing fast, intermediate, or slow photodegradation (Fig. 3). For slowly photodegrading compounds (first-order rate constant $k < 10^{-2}\ d^{-1}$), reaction with $^{\bullet}OH$ is often the main photodegradation pathway, presumably because the highly-reactive hydroxyl radical is the PPRI with the highest ability to abstract H atoms from C—H bonds. Such bonds are actually the

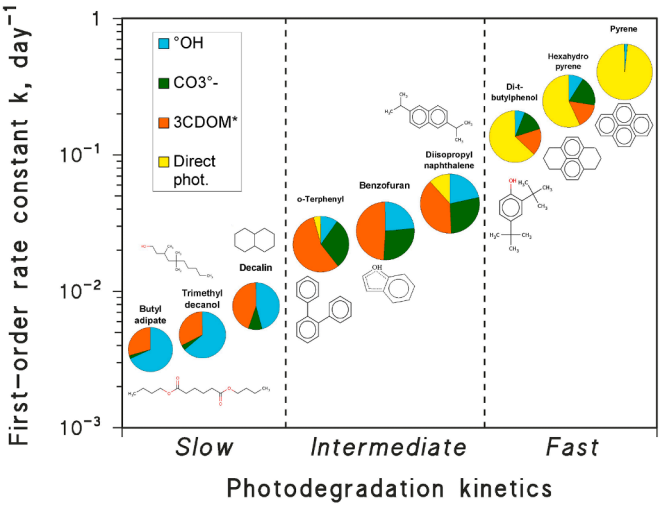

Fig. 3. Modeled photodegradation rate constants *k* of sample compounds that show slow, intermediate, or fast photodegradation kinetics. Model conditions: 3 m depth, 3 $mg_C\ L^{-1}$ DOC, 10^{-4} M NO_3^-, 10^{-6} M NO_2^-, 10^{-3} M HCO_3^-, and 10^{-5} M CO_3^{2-}; year-round average values at mid latitude.

Table 2
Ratios of predicted environmental concentrations (PEC_{light}/PEC_{dark}), predicted no effect concentrations ($PNEC_{dark}/PNEC_{light}$), and relative Risk ratios with and without light, based on yearly-averaged light profile.

ID#	Substance	PEC ratio[1]	PNEC Ratio[2]	Risk Ratio[3]
1	decalin	0.88	1	0.88
2	3-methylphenanthrene	0.65	2.49	1.62
3	benzofuran	0.76	1.11	0.84
4	dicyclopentadiene	0.64	1	0.64
5	trimethyldecanol	0.96	1	0.96
6	dibutyladipate	0.96	1	0.96
7	alkylated anisole	0.64	1.43	0.92
8	2,4,6 tri-tert-butylphenol	0.28	2.52	0.71
9	4,4′ di-tert-butyl-diphenylamine	0.016	6.22	0.097
10	dodecahydrochrysene	0.64	1	0.64
11	dehydroabietine	0.44	1.61	0.72
12	2,6 diisopropylnaphthalene	0.61	2.48	1.52
13	hexahydropyrene	0.30	7.30	2.17
14	o-terphenyl	0.73	1.1	0.80
15	dihydrodicyclopentadiene	0.48	1	0.48
16	bicyclo[4.1.0]heptane-7-ylidenecyclopentane	0.30	1	0.30
17	tris(4-isopropylphenyl)-phosphate	0.88	1	0.89
18	2,4-di-tert-butylphenol	0.24	3.16	0.77
19	triisononyl trimellitate	0.32	1.93	0.62
20	tetradecylnaphthalene	0.55	2.94	1.61
21	anthracene	0.13	26.1	3.33
22	fluoranthene	0.75	22.7	17.1
23	pyrene	0.16	20.5	3.24
24	benzo[a]pyrene	0.053	49.3	2.61
25	dibenzothiophene	0.74	2.55	1.89

[1] (Light / Dark, Eq. (4)).
[2] (Dark / Light, inverse of Eq. (3)).
[3] (Eq. (4) / Eq. (3)).

main attack sites for oxidation of saturated compounds with few or no other functionalities (Gligorovski et al., 2015; Minakata et al., 2009). In the case of electron-rich organic compounds which display intermediate photodegradation kinetics ($k = 10^{-2} - 10^{-1}$ d^{-1}), the different photoreaction pathways appear to play roughly comparable roles, in accordance with the reactivity/selectivity principle. Direct photolysis is the prevailing pathway for the compounds exhibiting the fastest rates ($k > 10^{-1}$ d^{-1}) as this pathway requires no PPRIs. The predicted ordering of photodegradation rates followed by the investigated compounds (phenols/anilines ~ PAHs > monoaromatics ~ olefins > saturated aliphatics, see Fig. A2) is consistent with previous investigations of the environmental photodegradation kinetics of these classes of molecules, for which photoreactivity details have been thoroughly elucidated by means of dedicated experimental measurements (Vione, 2020).

3.3. Role of light on simulated aquatic exposures

The overall degradation rates, with and without photodegradation, were evaluated using a one compartment model (Eq. (4)) to calculate exposure based on an assumed residence time of water considered typical of northern Europe (43.3 days). The relative change was evaluated as the ratio, PEC_{light}/PEC_{dark}, of the PEC based on biodegradation as well as direct and indirect photodegradation (PEC_{light}) to the PEC based only on biodegradation (PEC_{dark}). In this framework, the PEC_{light}/PEC_{dark} ratio for the chemicals in the present study that are strongly affected by photodegradation will be less than one, and those chemicals that have minimal direct or indirect photolysis will have ratios near 1. The results are provided in Table 2, and Fig. 4, panel A.

Decalin, trimethyldecanol, and dibutyladipate exhibit PEC_{light}/PEC_{dark} ratios near 1, consistent with their low photoreactivity (Fig 4 Panel A, Fig 3). Aromatic molecules like 3-methylphenanthrene or alkylated anisole show moderate interactions with PEC_{light}/PEC_{dark} ratios near 0.6. On the other hand, the PEC_{light}/PEC_{dark} ratios of certain PAHs (pyrene, benzo[a]pyrene, anthracene), 4,4′ di-*tert*-butyldiphenylamine, and the tert-butyl phenols are strongly affected by light, exhibiting PEC ratios ranging from 0.016 to 0.16. The PEC_{light}/PEC_{dark} ratios reflect influences from both the direct and indirect photodegradation, because the biodegradation rates are assumed to be the same in both scenarios. As noted above (Fig 2, 3) the direct photolysis rates are the dominant process controlling the PECs for several molecules that are susceptible to direct photodegradation.

3.4. Role of light on photosensitization

The role of light absorption on the toxicity thresholds (PNEC) was evaluated in a similar manner as the PECs. However, the ratio is reversed so that enhanced toxicity under irradiation corresponds to an increase in the PNEC ratios (Fig 4B, Table 2). The technical basis for the toxicity model is also related to the absorption of photons (Pabs) but also modified through calibration to empirical data (Eq. (3)). In Fig. 4B the $PNEC_{dark}/PNEC_{light}$ ratios are compared to the product of Pabs and QY, and molecules that do not absorb light have a ratio of exactly 1 (e.g., no difference). Since photon absorption is the key event, only molecules that absorb light have PNECs that are affected by light.

It is observed that the $PNEC_{dark}/PNEC_{light}$ ratios increase with increasing Pabs*QY (Fig 4B), and for generally the same molecules that are observed to undergo photodegradation (e.g., PEC ratios < 1, Fig 4A). The X-axis metric (QY * Pabs) is mechanistically related to direct photolysis (Eqs. (1, 2)) and appears mechanistically related to photosensitization since the other parameters around the Pabs term approximate a QY of toxicity (Eq. (3)). One notable outlier is fluoranthene (ID 22, Table 2) which shows a $PNEC_{dark}/PNEC_{light}$ ratio near 23 indicating strong photosensitization, but has a low PEC_{light}/PEC_{dark} ratio (near 0.8) indicating low susceptibility for photodegradation. In this framework, these results can be explained if the mechanism of phototoxicity of fluoranthene is relatively potent and involves the formation of highly toxic photoproduct molecules within an organism.

3.5. Impact of photodegradation on estimated risk

The combined impact of light on Risk (e.g., PEC / PNEC) was estimated as the product of the Ratio of PECs (PEC_{light}/PEC_{dark}, Eq. (4)) and

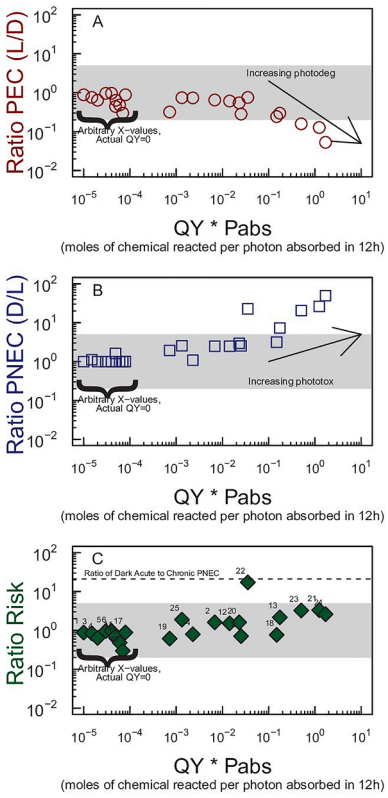

Fig. 4. Comparing the relative predicted exposure concentrations (PEC, open circles, A) in Light vs Dark (PEC_{light}/PEC_{dark}), the relative predicted no effect concentration (PNEC, open squares, B) in Dark vs Light ($PNEC_{dark}/PNEC_{light}$), and the relative change in Risk ((PEC_{light}/PEC_{dark}) * ($PNEC_{dark}/PNEC_{light}$), filled diamonds, C) against the product of the quantum yield (QY) and the photon absorption (Pabs) over a 12 h period. Results are for light intensity at Torino, Italy (year-round average). Grey band represents a factor of 5 around the model predictions. Chemical ID numbers are provided in panel C (see Table 2).

the Ratio of PNECs ($PNEC_{dark}/PNEC_{light}$, inverse of Eq. (3)). For the purposes of the present study "Light" refers to scenarios with photodegradation or photosensitization and the term "Dark" refers to a scenario without photodegradation or photosensitization. Ratios of the Risk (i.e., a ratio of ratios) greater than 1 suggest that the role of light on fate and toxicity increases the predicted risk in this hypothetical scenario. The results of the present study are given as green diamonds in Fig. 4C. The antioxidants (4,4′ di-*tert*-butyl-diphenylamine and tert-butyl phenols) and bicyclo[4.1.0]heptane-7-ylidenecyclopentane exhibit risk ratios substantially less than 1, ranging from 0.097 to 0.34, which is consistent with their function as anti-oxidants (Rudnick, 2009). In general the estimated risk ratios are near one because the phototoxicity is mitigated by the reduced exposure resulting from photodegradation. According to this analysis, the phenols, and other mono-aromatic constituents, show lower relative risk, because of their relative high photolysis rates due to their relatively high quantum yields (Table S2), and low phototoxicity profiles consistent with their usage as anti-oxidants in petrochemicals.

The evaluation strategy in the present study relies on a series of models to predict the direct and indirect photodegradation and phototoxicity in aquatic systems. Each of the models are based on mechanistic principles, calibrated to empirical data, which have associated variability around the predictions. The performance of the photodegradation and photosensitization model predictions is described as order of magnitude accuracy (Marzooghi et al., 2017; Vione, 2020). Propagation of error was not systematically evaluated so qualitative thresholds are given of +/- factor of 5 with results intended to provide general trends.

This analysis highlights the complexity that light can introduce to screening-level risk assessments, and the series of modeling calculations provided here forms the basis of a refined analysis considering both phototoxicity and photodegradation. In this analysis, risk estimates across all test substances were found to be within an order of magnitude of estimates derived ignoring light. Further, since risk assessments typically involve chronic endpoints, the typical hazard assessment approach is expected to provide sufficient conservatism to address photo-enhanced toxicity even for photoreactive chemicals. Thus, including the additional complexity of light interactions within substance risk assessments adds the most practical benefit for informing risk management decisions in cases of light-susceptible structures such as chromophores or antioxidants. To illustrate we compare the calculated relative photo-risk ratios to the calculated ratio of dark acute to dark chronic (conventional) PNECs (the dashed line in Fig. 4C). Even for a molecule like fluoranthene, which shows limited photodegradation rates and relative high photo toxicity, the conventional chronic PNECs are protective of the apparent photo-enhanced risk ratios.

Phototransformation products were not assessed in the present study, in some cases the photoproducts are less toxic than the parent molecules such as with PAH (Nordborg et al., 2023) but other antioxidant molecules may form reactive intermediates that could be more potent than the parent molecules. For example, the tire antioxidant, 6PPD, can form an ecotoxic quinone by reaction with tropospheric ozone (Zhao et al., 2023). For antioxidant molecules additional evaluation of phototransformation products may be needed to characterize the formation, toxicity, and stability of the intermediates.

3.6. *Role of seasonality*

The light spectra and intensity vary by month and were used to characterize the seasonal variation of light on the predicted exposures, toxicity thresholds, and risk (Table S2). General seasonal trends in the PPRI are shown in Fig. A3 (Appendix A5). Seasonality may also affect other processes such as biodegradation, but biodegradation rates were in the present study not modified by month to focus the attention on the role of light. Three example constituents are given in Fig. 5 to illustrate the role of season on the predicted PEC, PNEC, and Risk ratios. The example constituents (decalin, anthracene, and a substituted phenol) are generally representative of the range of structure and function of the chemicals in the present study. For example, decalin is a cyclic alkane found in fuels and solvents, which is not photoactive but is susceptible to indirect photodegradation. Anthracene is a widely recognized photoactive polycyclic aromatic hydrocarbon, which is subject to photo enhanced toxicity and direct and indirect photodegradation. The antioxidant, 2,4-di-tert-butylphenol, has aromatic features, which absorb light and undergo photodegradation and phototoxicity.

Decalin (Top row Fig. 5) shows little seasonal variation because of the lack of direct photolysis (zero photons absorbed), and its minor response to the indirect photodegradation (March, 1.1×10^{-2} d^{-1}), which is slower than the estimated biodegradation rate (5.7×10^{-2} d^{-1}), Table S7. Therefore, the PEC (right panel, top row, Fig. 5) ratios show little variation by month with a slight decrease in the summer months, when higher irradiance results in relatively higher formation of PPRI that enhance indirect photodegradation. The PNEC ratios do not change by month because Decalin does not absorb photons (middle panel, top row, Fig. 5).

Anthracene (middle row, Fig. 5), in contrast shows substantial impact of both photodegradation and phototoxicity consistent with strong estimated absorption of photons (~415 mol photons / mol chemical in 12 h period, annual average, Table S5). The higher photon absorption results in much faster direct photolysis rates (0.2 – 3.3 d^{-1}), Table S7. With this example it is apparent that the shape of the PNEC ratios are less variable across months, in contrast to the PEC ratios, which show a steeper variation by month, with less impact observed in the winter months. This is due to the formulation of the respective

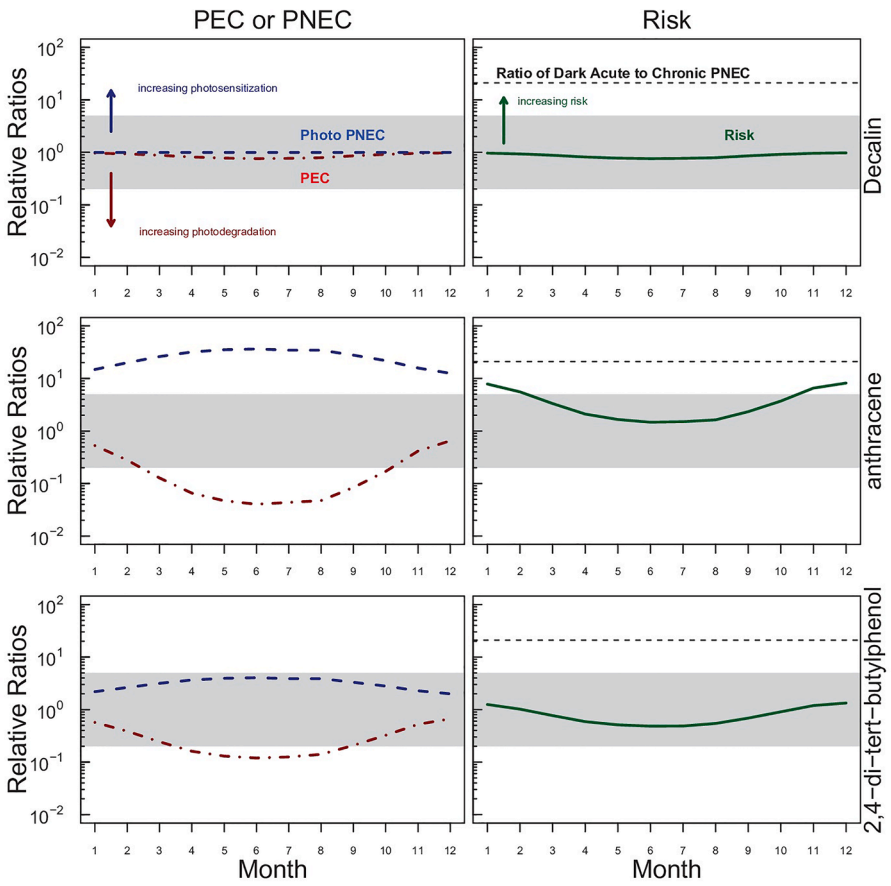

Fig. 5. *First column:* Comparing the relative impact of light on the predicted exposure concentrations (PEC_{light}/PEC_{dark}, dot-dash red line, Eq (4)), and the relative impact of light on the predicted no effect concentrations ($PNEC_{dark}/PNEC_{light}$, dashed blue line, inverse of Eq (3)). *Second Column:* The relative impact on Risk (Ratio Risk = Ratio PEC * Ratio PNEC, solid green line), and the ratio of acute thresholds to chronic thresholds without light (horizontal dashed line). Data presented for three example chemicals: Decalin, a dicyclic aliphatic molecule; anthracene, a photoactive three-ring aromatic hydrocarbon; 2,4-di-tert-phenol, a substituted phenol often used as an anti-oxidant in petrochemical substances.

toxicity and degradation models. Specifically, direct photolysis is linear with respect to the light (e.g., photon absorption) according to Eq. (1). The ratios of PEC and PNEC both scale with Pabs (Fig 5, middle row, right panel), but the slope of the PNEC and Pabs based on the photo-toxicity model, Eq. (3), uses an exponential power term α of 0.426 on the absorbed photons term, which means the impact of light on toxicity is less variable between months. The summer months show a greater impact on the exposure (e.g., lower PEC) and toxicity (greater PNEC). In the winter months, both metrics show a lower impact of light consistent with the lower irradiance.

The antioxidant, 2,4-di-*tert*-butyl phenol exhibits a substantial impact of photodegradation, which results in relative Risk ratios that are less than one (Fig. 5, bottom row). During the summer months the impact of photodegradation is substantial, showing approximately an order of magnitude lower ratios in PECs. The substituted phenol absorbed approximately 2.5 photons / molecule of chemical over 12 h in this simulation, which is substantially less than the absorption estimated for anthracene and other PAH. However, the QY for this molecule is two orders of magnitude greater than the PAH (0.33 vs <0.003, Table S3), which results in similar direct photolysis rates for phenols relative to PAH (Table S7). However, the reduced photon absorption results in less photoenhanced toxicity, so that the predicted risk ratios are less than one, indicating that photodegradation is a more important process than phototoxicity for phenols. The slopes between the PEC and PNEC ratios and Pabs for the phenol are similar to those observed for anthracene. However, it is substantially offset toward the left indicating a more efficient reaction at lower photon absorption, consistent with the higher QY. The PNEC ratios are also lower than anthracene due to the lower Pabs of the phenol constituent.

4. Discussion

The interaction of light with organic chemicals is complex and is a function of both the spectra and intensity of the light source, the molecular absorption properties of the organic chemicals, and the effective quantum yields for photodegradation and toxicity. In addition, the role of indirect photodegradation can be an important process based on the interaction of light with common constituents found in water such as dissolved organic matter and nitrate. In the present study, state of the art mechanistic models were used to estimate the relative impacts of light on degradation and toxicity in a screening-model analysis with representative environmental conditions.

Toxicity and photodegradation both vary with light intensity, and the specific impacts vary by chemical class. Non-aromatic constituents that do not absorb light can still undergo indirect photodegradation processes, while for compounds where indirect photochemistry combines with direct photodegradation, the result is a decrease in the PECs by up to an order of magnitude under the conditions of the present modeling study. Phenolic antioxidants in particular exhibit a predicted reduction on the PECs and corresponding reduction of the calculated risk in the presence of light which, however, does not consider potential risks arising from phototransformation products such as quinones (vide infra).

Within these assumptions, the calculated risk ratios can vary widely

between chemical classes, and seasonally. For some classes, like PAH, the calculated photorisk ratios can be substantial, even larger than the estimated uncertainty bands for the respective phototoxicity and photodegradation models. This suggests that in some circumstances the role of light should be considered explicitly, which requires compilation of specific properties of the light exposure such as intensity, spectra, and attenuation coefficients. In addition, the behavior and physiology of the organisms of interest could be relevant, as well as the chemical properties of absorption and quantum yields. It is assumed that phototoxicity is an acute toxicity phenomenon that is relevant mainly at high exposure concentrations and under shorter durations. Guidance is given in Alloy et al., (2023) for the types of data and analytical techniques that are used to characterize light intensity, etc. Therefore, an intermediate step in a risk assessment might include the comparison of exposure concentrations to the PNECs for chronic endpoints (Parkerton et al., 2023). As demonstrated in Figs. 4 and 5, the conventional chronic PNEC would be protective of the calculated photoenhanced risks.

A general conclusion from the present study is that photochemical transformation (direct and indirect) of organic chemicals can be an important fate process, altering the predicted environmental effect concentrations by up to an order of magnitude beyond typical biodegradation processes. The result of the combined risk assessment was that the enhanced removal by photodegradation generally mitigated the enhanced photosensization.

Future work can include consideration of potentially toxic phototransformation products from certain chemical classes like antioxidants. In addition, evaluation under different water quality characteristics could be done for different regions and exposure scenarios. Further, study of chronic phototoxicity could be done to understand the role of organism recovery and avoidance mechanisms in different exposure scenarios. It should also be underlined that this approach might be applied to a range of over 40 emerging contaminants (mostly pesticides, pharmaceuticals, and personal care products) for which experimental data of photodegradation kinetics are available, which enables their photochemical modeling (Vione, 2020).

5. Conclusions

- Photochemical degradation is often not incorporated in substance risk assessments, usually due to lack of data to predict photodegradation kinetics.
- In this work, for the first time, we have predicted photochemical reactivity and incorporated photochemical processes in screening-level risk assessments for 25 petrochemical structures with varied uses and environmental fate properties.
- We compared the ratios of predicted exposure concentrations with and without light to the corresponding ratios of toxicity thresholds, assessing how inclusion of light modulates substance risk analysis.
- Inclusion of light decreased PECs as a result of photodegradation and decreased PNECs due to photoenhanced toxicity caused by photosensitization, thereby altering risk quotients. In many cases, the predicted increase in substance hazard (photoenhanced toxicity) was mitigated by the reduction in exposure. For many structures, indirect photodegradation would decrease environmental exposures independently of the direct photolysis pathway, which is associated with enhanced phototoxicity for most of the scenarios and chemicals of the present work.

CRediT authorship contribution statement

Davide Vione: Writing – review & editing, Writing – original draft, Software, Formal analysis, Data curation, Conceptualization. **J. Samuel Arey:** Writing – review & editing, Software, Investigation, Conceptualization. **Thomas F. Parkerton:** Writing – review & editing, Validation, Investigation, Formal analysis, Data curation. **Aaron D. Redman:** Writing – review & editing, Writing – original draft, Supervision, Resources, Methodology, Investigation, Conceptualization.

Declaration of competing interest

The authors declare that they have no known competing financial interests or personal relationships that could have appeared to influence the work reported in this paper.

Data availability

Data will be made available on request.

Acknowledgements

Craig Davis provided biodegradation rate calculations. Lesheng Wang collected molar absorption values.

Supplementary Material available

A pdf file containing the Appendix (cited here as Text A#, Table A#) and a xls file with the supplementary tables (each indicated as Table S#).

Supplementary materials

Supplementary material associated with this article can be found, in the online version, at doi:10.1016/j.watres.2024.121677.

References

Albanese, K.A., Lanno, R.P., Hadad, C.M., Chin, Y.-P., 2017. Photolysis- and dissolved organic matter-induced toxicity of triclocarban to daphnia magna. Environ. Sci. Technol. Lett. 4 (11), 457–462.

Alloy, M.M., Finch, B.E., Ward, C.P., Redman, A.D., Bejarano, A.C., Barron, M.G., 2023. Recommendations for advancing test protocols examining the photo-induced toxicity of petroleum and polycyclic aromatic compounds. Aquat. Toxicol., 106390

Ankley, G.T., Erickson, R.J., Sheedy, B.R., Kosian, P.A., Mattson, V.R., Cox, J.S., 1997. Evaluation of models for predicting the phototoxic potency of polycyclic aromatic hydrocarbons. Aquat. Toxicol. 37 (1), 37–50.

Arnold, W.A., Oueis, Y., O'Connor, M., Rinaman, J.E., Taggart, M.G., McCarthy, R.E., Foster, K.A., Latch, D.E., 2017. QSARs for phenols and phenolates: oxidation potential as a predictor of reaction rate constants with photochemically produced oxidants. Environ. Sci. Process. Impacts 19 (3), 324–338.

Bianco, A., Fabbri, D., Minella, M., Brigante, M., Mailhot, G., Maurino, V., Minero, C., Vione, D., 2015. New insights into the environmental photochemistry of 5-chloro-2-(2, 4-dichlorophenoxy) phenol (triclosan): reconsidering the importance of indirect photoreactions. Water Res. 72, 271–280.

Björn, L.O., Huovinen, P., 2015. Phototoxicity. Photobiol. Sci. Light Life 335–345.

Bodrato, M., Vione, D., 2014. APEX (Aqueous photochemistry of environmentally occurring xenobiotics): a free software tool to predict the kinetics of photochemical processes in surface waters. Environ. Sci. Process. Impacts 16 (4), 732–740.

Bonvin, F., Razmi, A.M., Barry, D.A., Kohn, T., 2013. Micropollutant dynamics in Vidy Bay—A coupled hydrodynamic-photolysis model to assess the spatial extent of ecotoxicological risk. Environ. Sci. Technol. 47 (16), 9207–9216.

Boreen, A.L., Arnold, W.A., McNeill, K., 2003. Photodegradation of pharmaceuticals in the aquatic environment: a review. Aquat. Sci. 65, 320–341.

Brezonik, P.L., Fulkerson-Brekken, J., 1998. Nitrate-induced photolysis in natural waters: controls on concentrations of hydroxyl radical photo-intermediates by natural scavenging agents. Environ. Sci. Technol. 32 (19), 3004–3010.

CONCAWE (2013) Challenges in addressing phototoxicity and photodegradation in the environmental risk assessment of polycyclic aromatic hydrocarbons in the aquatic compartment, p. 37, Brussels BE.

CONCAWE (2020) Assessment of photochemical processes in environmental risk assessment of PAHs, p. 47, Brussels BE.

Davis, C.W., Camenzuli, L., Redman, A.D., 2022. Predicting primary biodegradation of petroleum hydrocarbons in aquatic systems: integrating system and molecular structure parameters using a novel machine-learning framework. Environ. Toxicol. Chem. 41 (6), 1359–1369.

Den Hollander, H., Van Eijkeren, J., Van de Meent, D, 2004. SimpleBox 3.0: multimedia mass balance model for evaluating the fate of chemicals in the environment. Bilthoven (NL) Natl. Inst. Public Health Environ. (RIVM). Report 601200003.

Fasnacht, M.P., Blough, N.V., 2003. Kinetic analysis of the photodegradation of polycyclic aromatic hydrocarbons in aqueous solution. Aquat. Sci. 65 (4), 352.

Finch, B.E., Marzooghi, S., Di Toro, D.M., Stubblefield, W.A., 2017. Phototoxic potential of undispersed and dispersed fresh and weathered Macondo crude oils to Gulf of Mexico marine organisms. Environ. Toxicol. Chem. 36 (10), 2640–2650.

Gligorovski, S., Strekowski, R., Barbati, S., Vione, D., 2015. Environmental implications of hydroxyl radicals (• OH). Chem. Rev. 115 (24), 13051–13092.
Guerard, J.J., Chin, Y.-P., Mash, H., Hadad, C.M., 2009. Photochemical fate of sulfadimethoxine in aquaculture waters. Environ. Sci. Technol. 43 (22), 8587–8592.
Janssen, E.M.-L., Erickson, P.R., McNeill, K., 2014. Dual roles of dissolved organic matter as sensitizer and quencher in the photooxidation of tryptophan. Environ. Sci. Technol. 48 (9), 4916–4924.
Jasper, J.T., Sedlak, D.L., 2013. Phototransformation of wastewater-derived trace organic contaminants in open-water unit process treatment wetlands. Environ. Sci. Technol. 47 (19), 10781–10790.
Kang, H.-J., Jung, Y., Kwon, J.-H., 2019. Changes in ecotoxicity of naphthalene and alkylated naphthalenes during photodegradation in water. Chemosphere 222, 656–664.
Latch, D.E., Packer, J.L., Stender, B.L., VanOverbeke, J., Arnold, W.A., McNeill, K., 2005. Aqueous photochemistry of triclosan: formation of 2,4-dichlorophenol, 2,8-dichlorodibenzo-p-dioxin, and oligomerization products. Environ. Toxicol. Chem. 24 (3), 517–525.
Loiselle, S., Vione, D., Minero, C., Maurino, V., Tognazzi, A., Dattilo, A.M., Rossi, C., Bracchini, L., 2012. Chemical and optical phototransformation of dissolved organic matter. Water Res. 46 (10), 3197–3207.
Mackay, D., 2001. Multimedia Environmental models: the Fugacity Approach. CRC press.
Magazinovic, R.S., Nicholson, B.C., Mulcahy, D.E., Davey, D.E., 2004. Bromide levels in natural waters: its relationship to levels of both chloride and total dissolved solids and the implications for water treatment. Chemosphere 57 (4), 329–335.
Mansouri, K., Grulke, C.M., Judson, R.S., Williams, A.J., 2018. OPERA models for predicting physicochemical properties and environmental fate endpoints. J. Cheminform. 10 (1), 1–19.
Marzooghi, S., Di Toro, D.M., 2017. A critical review of polycyclic aromatic hydrocarbon phototoxicity models. Environ. Toxicol. Chem. 36 (5), 1138–1148.
Marzooghi, S., Finch, B.E., Stubblefield, W.A., Di Toro, D.M., 2018. Predicting phototoxicity of alkylated PAHs, mixtures of PAHs, and water accommodated fractions (WAF) of neat and weathered petroleum with the phototoxic target lipid model. Environ. Toxicol. Chem. 37 (8), 2165–2174.
Marzooghi, S., Finch, B.E., Stubblefield, W.A., Dmitrenko, O., Neal, S.L., Di Toro, D.M., 2017. Phototoxic target lipid model of single polycyclic aromatic hydrocarbons. Environ. Toxicol. Chem. 36 (4), 926–937.
McGrath, J.A., Fanelli, C.J., Di Toro, D.M., Parkerton, T.F., Redman, A.D., Paumen, M.L., Comber, M., Eadsforth, C.V., den Haan, K., 2018. *Re*-evaluation of target lipid model–derived HC5 predictions for hydrocarbons. Environ. Toxicol. Chem. 37 (6), 1579–1593.
McNeill, K., Canonica, S., 2016. Triplet state dissolved organic matter in aquatic photochemistry: reaction mechanisms, substrate scope, and photophysical properties. Environ. Sci. Process. Impacts 18 (11), 1381–1399.
Minakata, D., Li, K., Westerhoff, P., Crittenden, J., 2009. Development of a group contribution method to predict aqueous phase hydroxyl radical (HO•) reaction rate constants. Environ. Sci. Technol. 43 (16), 6220–6227.
Minero, C., Chiron, S., Falletti, G., Maurino, V., Pelizzetti, E., Ajassa, R., Carlotti, M.E., Vione, D., 2007. Photochemincal processes involving nitrite in surface water samples. Aquat. Sci. 69 (1), 71–85.
Nordborg, F.M., Brinkman, D.L., Fisher, R., Parkerton, T.F., Oelgemöller, M., Negri, A.P., 2023. Effects of aromatic hydrocarbons and evaluation of oil toxicity modelling for larvae of a tropical coral. Mar. Pollut. Bull. 196, 115610.
Parkerton, T.F., French-McCay, D., de Jourdan, B., Lee, K., Coelho, G., 2023. Adopting a toxic unit model paradigm in design, analysis and interpretation of oil toxicity testing. Aquat. Toxicol. 255, 106392.
Reinart, A., Paavel, B., Tuvikene, L., 2004. Effect of coloured dissolved organic matter on the attenuation of photosynthetically active radiation in Lake Peipsi. Proc. Estonian Acad. Sci. Biol. Ecol. 53 (2), 88–105.
Remucal, C.K., 2014. The role of indirect photochemical degradation in the environmental fate of pesticides: a review. Environ. Sci. Process. Impacts 16 (4), 628–653.
Rosario-Ortiz, F.L., Canonica, S., 2016. Probe compounds to assess the photochemical activity of dissolved organic matter. Environ. Sci. Technol. 50 (23), 12532–12547.
Rudnick, L.R. (2009) Lubricant Additives: Chemistry and Applications, Taylor & Francis.
Schwarzenbach, R.P., Gschwend, P.M., Imboden, D.M., 2016. Environmental Organic Chemistry. John Wiley & Sons.
Sellin Jeffries, M.K., Claytor, C., Stubblefield, W., Pearson, W.H., Oris, J.T, 2013. Quantitative risk model for polycyclic aromatic hydrocarbon photoinduced toxicity in Pacific herring following the Exxon Valdez oil spill. Environ. Sci. Technol. 47 (10), 5450–5458.
Soltermann, F., Abegglen, C., Götz, C., von Gunten, U., 2016. Bromide sources and loads in Swiss surface waters and their relevance for bromate formation during wastewater ozonation. Environ. Sci. Technol. 50 (18), 9825–9834.
Van de Meent, D., McKone, T., Parkerton, T., Matthies, M., Scheringer, M., Wania, F., Purdy, R., Bennett, D., 2000. Persistence and Transport Potential of Chemicals in a Multimedia Environment. Lawrence Berkeley National Lab.(LBNL), Berkeley, CA (United States).
Vione, D., 2020. A critical view of the application of the APEX software (aqueous photochemistry of environmentally-occurring xenobiotics) to predict photoreaction kinetics in surface freshwaters. Molecules. 25 (1), 9.
Vione, D., Carena, L., 2022. Direct photolysis of contaminants in surface freshwaters, within the equivalent monochromatic wavelength (EMW) approximation. Chemosphere 307, 135982.
Vione, D., Das, R., Rubertelli, F., Maurino, V., Minero, C., Barbati, S., Chiron, S., 2010. Modelling the occurrence and reactivity of hydroxyl radicals in surface waters: implications for the fate of selected pesticides. Int. J. Environ. Anal. Chem. 90 (3–6), 260–275.
Vione, D., Minero, C., Housari, F., Chiron, S., 2007. Photoinduced transformation processes of 2,4-dichlorophenol and 2,6-dichlorophenol on nitrate irradiation. Chemosphere 69 (10), 1548–1554.
Vione, D., Scozzaro, A., 2019. Photochemistry of surface fresh waters in the framework of climate change. Environ. Sci. Technol. 53 (14), 7945–7963.
Ward, C.P., Sharpless, C.M., Valentine, D.L., French-McCay, D.P., Aeppli, C., White, H.K., Rodgers, R.P., Gosselin, K.M., Nelson, R.K., Reddy, C.M., 2018. Partial photochemical oxidation was a dominant fate of Deepwater Horizon surface oil. Environ. Sci. Technol. 52 (4), 1797–1805.
Werner, J.J., McNeill, K., Arnold, W.A., 2005. Environmental photodegradation of mefenamic acid. Chemosphere 58 (10), 1339–1346.
Williamson, C.E., Fischer, J.M., Bollens, S.M., Overholt, E.P., Breckenridge, J.K., 2011. Toward a more comprehensive theory of zooplankton diel vertical migration: integrating ultraviolet radiation and water transparency into the biotic paradigm. Limnol. Oceanogr. 56 (5), 1603–1623.
Williamson, C.E., Neale, P.J., Grad, G., De Lange, H.J., Hargreaves, B.R., 2001. Beneficial and detrimental effects of UV on aquatic organisms: implications of spectral variation. Ecol. Appl. 11 (6), 1843–1857.
Yan, S., Liu, Y., Lian, L., Li, R., Ma, J., Zhou, H., Song, W., 2019. Photochemical formation of carbonate radical and its reaction with dissolved organic matters. Water Res. 161, 288–296.
Yan, S., Song, W., 2014. Photo-transformation of pharmaceutically active compounds in the aqueous environment: a review. Environ. Sci. Process. Impacts 16 (4), 697–720.
Zeng, T., Arnold, W.A., 2013. Pesticide photolysis in prairie potholes: probing photosensitized processes. Environ. Sci. Technol. 47 (13), 6735–6745.
Zhao, H.N., Hu, X., Tian, Z., Gonzalez, M., Rideout, C.A., Peter, K.T., Dodd, M.C., Kolodziej, E.P., 2023. Transformation products of tire rubber antioxidant 6ppd in heterogeneous gas-phase ozonation: identification and environmental occurrence. Environ. Sci. Technol. 57 (14), 5621–5632.